Chemical Engineering Journal 162 (2010) 480–486

Contents lists available at ScienceDirect

Chemical Engineering Journal

journal homepage: www.elsevier.com/locate/cej

Kinetic assessment on the autohydrolysis of pectin-rich by-products

Martina Martínez, Beatriz Gullón, Remedios Yáñez, José Luis Alonso*, Juan Carlos Parajó

Department of Chemical Engineering, Faculty of Science, University of Vigo (Campus Ourense), As Lagoas, 32004 Ourense, Spain

ARTICLE INFO

Article history:
Received 31 March 2010
Received in revised form 24 May 2010
Accepted 25 May 2010

Keywords:
Sugar beet pulp
Pectin
Autohydrolysis
Kinetic modeling
Pectic-oligosaccharides
Oligogalacturonides
Arabinooligosaccharides

ABSTRACT

Fractionation in aqueous media is an environmentally friendly technology suitable for obtaining oligomeric products from pectins and hemicelluloses. Sugar beet pulp (SBP) samples were subjected to aqueous processing under non-isothermal conditions to reach maximal temperatures in the range 140–200 °C, in order to cause the conversion of pectins into soluble compounds of lower molecular weight with potential applications as prebiotic ingredients.

Mixtures of arabinooligosaccharides, oligogalacturonides and oligomers made up of other structural units were obtained by non-isothermal processing of SBP in aqueous media. Kinetic models suitable for reproducing and predicting compositional data of reaction liquors as a function of the operational conditions were developed. According to the model predictions, the maximum arabinooligosaccharides yield (15.7 g/100 g SBP) corresponded to a treatment carried out to achieve 171.5 °C. Alternatively, the maximum oliogogalacturonide yield (14.1 g/100 g SBP) was predicted for a treatment performed to achieve 158.2 °C. In both cases, the overall yield of oligomeric saccharides was near to 30 g/100 g dry SBP, whereas the oligosaccharide mixture of higher purity was obtained operating at 158.2 °C. Depending on the operational conditions, SBP processing in aqueous media yielded oligomers with different compositional profiles. The developed models were suitable for a quantitative interpretation of experimental data, and provided key information for both design calculations and economic evaluation.

1. Introduction

The demand of functional ingredients with improved properties has increased in the past few years [1]. The fast growth of the functional food market and the high selling price of prebiotic compounds fosters the search for new raw materials. Alternative, environmentally friendly technologies may play a significant role in the manufacture of new prebiotic ingredients.

Recent studies reported promising perspectives for pectin and pectin-derived oligosaccharides [1–3]. Pectin, a key polymer of vegetal raw materials, includes a family of polysaccharides with common features, but extremely diverse fine structures [4]. Thus, pectin is mainly made up of three structural elements: homogalacturonan (HG), rhamnogalacturonan I (RG-I) and rhamnogalacturonan II (RG-II). HG consists of a backbone of α-(1→4)-linked galacturonic acid (GalA) residues, which can be partially methyl-esterified at C-6 and acetyl-esterified at O-2 and/or O-3. RG-I is a ramified polymer made up of chains containing alternate units of galacturonic acid and rhamnose, where arabinan, galactan, arabinogalactan I and II branches can be attached. RG-II is a complex polymer composed of GalA, rhamnose, galactose and some unusual sugars. Fig. 1 shows a schematic representation of pectin, which is widely used as a gelling and stabilizing agent in food technology [5,6]. On the other hand, pectin has medical applications based on its health-promoting effects (including lowering of blood cholesterol and serum glucose levels, potential to cause inhibition of cancer growth and metastasis [7], and ability to modify the surfaces of medical materials [8]).

Currently, citrus peel and apple pomace are the major sources of pectin; whereas sugar beet pulp (SBP) is a potential alternative source. SBP is the spent solid resulting from sucrose extraction of sugar beet with hot water. Sugar beet is an important agricultural raw material, with a world production of 247 millions metric tons in 2007, of which 5.3 millions metric tons were produced in Spain [9]. In a typical sugar beet processing plant, 200 kg of wet SBP (75% (w/w) moisture) are produced from 1 ton of sugar beet. SBP is usually used as a low value component of animal feeds or disposed with an additional cost [10], and the importance of finding new applications for this by-product for the future profitability of the beet sugar processing industry has been pointed out [11].

Abbreviations: AcH, Acetic acid; Acn, Acetyl groups; AcO, Acetyl groups in oligomers; AOS, Arabinooligosaccharides; An, Arabinan; Ara, Arabinose; DP_i, Decomposition products (i = Gan, GaUn, An or Acn); F, Furfural; Gal, Galactose; GalA, Galacturonic acid; Gan, Galactan; GaOS, Galactooligosaccharides; GaUn, Galacturonan; HMF, Hydroxymethylfurfural; OGaU, Oligogalacturonides; OS, Total oligomers; SBP, Sugar beet pulp; Subscript "s", Susceptible fraction; Subscript "RM", Raw material; α_i, Mass fraction of susceptible polymer (i = Gan, GaUn or An).

* Corresponding author. Fax: +34 988 38 70 01.
E-mail address: xluis@uvigo.es (J.L. Alonso).

1385-8947/$ – see front matter © 2010 Elsevier B.V. All rights reserved.
doi:10.1016/j.cej.2010.05.048

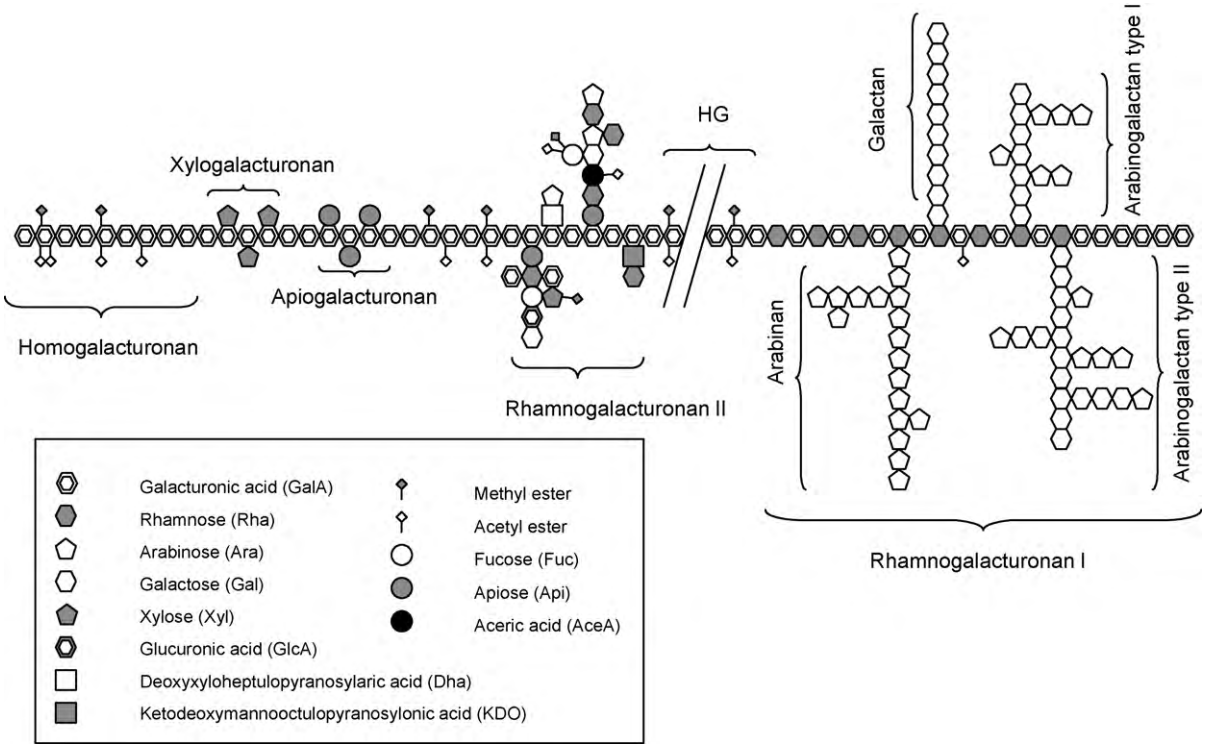

Fig. 1. Simplified structure of pectin.

In recent years, several applications of SBP were considered in literature, including bioethanol [12] or component of green composites [11]. Based on its high pectin content, mainly made up of HG and RG-I [4,13], research studies dealing with the manufacture and application of pectin-derived oligosaccharides have been conducted. Some considered topics include the enzymatic release of ferulic acid and the production of feruloylated oligosaccharides [14–16] or arabinooligosaccharides (AOS), as well as the prebiotic effects of pectin-derived oligomers [10,17].

In a recent work [18], our research group reported on the production pectic-oligomers from SBP by aqueous processing (hydrothermal or autohydrolysis treatments), a technology that shows some favorable features, including: (i) environmentally friendly character (water and feedstock are the only reagents), (ii) ability for generating oligosaccharides in a single stage at high yields, (iii) short reaction time, and (iv) simultaneous production of spent solids enriched in cellulose suitable for further utilization.

Optimization and scaling up of the controlled hydrolytic breakdown of pectic polymers requires the development of kinetic models suitable for predicting the composition of the reaction media achievable under defined operational conditions. To this end, kinetic models describing the non-isothermal autohydrolysis of SBP were developed. The models assumed the contributions of consecutive and parallel, pseudohomogeneous, first-order reactions, and enabled the calculation of media composition under conditions leading to the maximum production of galactooligosaccharides (GaOS), oligogalacturonides (OGaU), AOS or total oligomers (OS). To our knowledge, no studies dealing with the kinetic modeling of the autohydrolysis of pectin-rich materials have been reported.

2. Materials and methods

2.1. Raw material

SBP was supplied by a beet sugar processing industry (Azucarera Ebro, Spain), homogenized in a single lot to avoid compositional differences among aliquots and stored in polyethylene bags at −18 °C until use. Aliquots from this lot were subjected to analytical determinations according to the methodology described by Martínez et al. [18]. The composition (expressed in weight percent oven-dry basis) of the SBP lot used in this work was: 20.1% glucan (Gn), 5.3% galactan (Gan), 1% xylan, 1.4% rhamnosyl moieties, 1.1% mannan, 17.5% arabinan (An), 2.6% acetyl groups (Acn), 21% galacturonan (GaUn), 4.8% klason lignin, 4.5% ash and 10.8% protein.

2.2. Hydrothermal treatments

SBP samples were suspended in water (liquid to solid ratio = 12 g water/g oven-dry pulp) and reacted in a 3.75 L stainless steel reactor (Parr Instruments, Moine, IL, USA) under non-isothermal conditions following the standard heating temperature profile [18] to reach the desired temperatures (140, 150, 160, 163, 165, 167, 170, 180, 190 or 200 °C). At the end of treatments, the reactor was rapidly cooled (to achieve 60 °C), and the liquors were separated from spent solids by pressing. Solids were washed with distilled water and air-dried. Samples from liquors and spent solids were analyzed using the methodology described below.

2.3. Analytical methods

Samples of dried, spent solids were milled to a particle size below 0.5 mm and analyzed using the same methods employed for raw material characterization. Liquors from the quantitative acid hydrolysis of spent solids were analyzed for sugars and acetic acid (AcH) by HPLC using the method described by González-Muñoz et al. [19]. In HPLC chromatograms, galactose (Gal), xylose, mannose and rhamnose were eluted together. Since the Gal content of samples was considerably higher than the ones of the co-eluted sugars, the overall chromatographic peak was quantified and reported as Gal. Uronic acids in liquors were determined by the method of Blumenkrantz and Asboe-Hansen [20].

Table 1
Conversion yields (expressed as g of monomer equivalents/100 g of monomer equivalents in raw material).

Monomer/oligomer/polymer	T (°C)									
	140	150	160	163	165	167	170	180	190	200
Gal	5.3	1.8	24.1	25.9	29.0	32.8	34.0	35.2	36.7	32.7
GaOS	4.4	13.2	32.9	31.9	31.6	32.0	32.0	26.9	29.3	18.9
Gan (solid)	64.5	54.7	41.4	38.9	41.4	33.8	29.4	31.0	23.9	19.8
Ara	0.3	1.2	1.6	2.1	3.2	4.3	5.5	14.7	34.9	51.1
AOS	18.9	44.1	70.2	73.2	78.1	80.5	79.4	71.3	49.5	10.3
An (solid)	69.4	43.5	23.5	21.8	18.2	11.3	6.4	7.3	1.2	0.7
AcH	1.7	4.3	10.1	11.0	14.3	17.8	22.6	40.3	57.6	70.3
AcO	27.0	43.1	56.0	57.4	55.8	59.3	56.6	43.2	28.0	12.9
Acn (solid)	60.5	38.9	24.2	19.3	23.1	15.7	15.5	16.9	15.3	11.6
OGaU	34.7	47.0	56.8	51.9	47.9	45.9	41.8	20.5	6.9	3.4
GaUn (solid)	63.8	40.0	20.1	19.0	18.4	16.3	11.9	10.4	5.2	4.6

Samples of autohydrolysis liquors were filtered through 0.45 μm membranes and analyzed by HPLC for monosaccharides, furfural (F), hydroxymethylfurfural (HMF) and AcH. A second aliquot of each sample was subjected to quantitative posthydrolysis and analyzed by HPLC for AcO (acetyl groups attached to oligomers). Finally, a third aliquot of each sample was treated with an endo-polygalacturonase-rich enzymatic concentrate ("Viscozyme L" from *Aspergillus aculeatus*, kindly supplied by Novozymes, Madrid, Spain). The contents of oligomers (AOS, GaOS, OGaU) were calculated on the basis of the increase in each monomer concentration obtained upon quantitative hydrolysis of liquors. Additional information about the HPLC methodology and enzymatic assay conditions can be found elsewhere [18].

2.4. Kinetic model development

For calculation purposes, the experimental data employed for modeling were referred to the oven-dry weight of the raw material. The polymer contents were expressed as g/100 g dry raw material and other selected variables in terms of equivalent amounts per 100 g of dry raw material. Empirical equations were used to fit the temperature profiles and employed in the numerical solving of the differential equations listed in Section 3. The set of differential equations obtained from the proposed models was solved by the 4th order Runge–Kutta method. The preexponential factors and the activation energies were calculated by minimizing the sum of the deviation squares between experimental and calculated data. A commercial optimization routine dealing with the Newton's method (Solver, Microsoft Excel, Microsoft) was employed for this purpose. A set of variables were defined to measure the composition of the solid and the liquid fractions from autohydrolysis experiments (see list of abbreviations).

3. Results and discussion

3.1. Preliminary considerations

Starting from experimental data on the hydrothermal processing of SBP, this work deals with the development of kinetic models describing the major phenomena involved in pectin solubilization upon autohydrolysis. From the analytical data, balances to each polysaccharide fraction were calculated (see Table 1), and the variation patterns of the various fractions enabled the formulation of the proposed kinetic mechanism.

3.1.1. Galactan and galactan-derived products

From a quantitative point of view, galactose is one of the most important structural sugars of the rhamnogalacturonan type I, making part of galactan, arabinogalactan type I and arabinogalactan type II (see Fig. 1). According to the data in Table 1, the percentage of galactan (Gan) remaining in solid phase decreased with temperature to achieve a minimum near 20%, confirming the existence of a fraction of Gan not susceptible to hydrolysis under the conditions considered in this work. The percentage of Gan converted into GaOS first increased with temperature, then achieved a plateau (about 32% for experiments performed at maximal temperatures in the range 160–170 °C), and finally decreased. On the other hand, the Gal yield achieved a maximum of 36.7% in the experiment carried out to reach 190 °C. All these observations are compatible with a mechanism involving sequential reactions of GaOS generation from Gan, followed by Gal generation from GaOS system. Additionally, it can be observed that the joint contribution of Gan remaining in solid phase, GaOS and Gal decreased with temperature, confirming the existence of Gal decomposition reactions.

3.1.2. Galacturonan and galacturonan-derived products

GalA is the major structural component of pectins. According to Ralet et al. [13], 90% of SBP GalA is in the HG fraction (see Fig. 1), and the rest belongs to RG-I and RG-II.

As it can be deduced from Table 1, even though GaUn showed high susceptibility to hydrolysis reactions, 4.6% of GaUn remained in solid phase after the treatment performed under the severest conditions assayed. OGaU showed a maximum (57% of GaUn) at 160 °C, and then decreased sharply. The joint contribution of GaUn and OGaU varied from 98.5% (at 140 °C) to 8% (at 200 °C), confirming the existence of decomposition reactions involving these species. As no GalA (in monomeric form) was detected in liquors, it can be postulated that OGaU are directly decomposed. GalA degradation was experimentally confirmed (data not shown) by heating commercial solutions of polygalacturonic acid and apple pomace pectin under non-isothermal conditions to reach final temperatures in the range of 180–205 °C.

3.1.3. Arabinan and arabinan-derived products

Arabinan is a pectic polysaccharide consisting of highly branched chains of arabinofuranoside residues, which accounts for 15–21 weight percent of the dry SBP [10]. However, arabinose is also present in other pectic polymers such as arabinogalactans I and II (Fig. 1). An was highly susceptible to the depolymerization reactions (it can be seen in Table 1, spent solids from the severest experiment was free from this fraction).

The maximum AOS yield (80.5%) was achieved in the experiment carried out to reach 167 °C. At higher temperatures, AOS were partially hydrolyzed to give Ara, whose yield increased steadily with the severity of treatments to achieve 51% at 200 °C. The joint contribution of Ara, AOS and residual An in solid phase decreased rapidly at temperatures above 165 °C, achieving of 62.2% in the experiment carried out to reach a maximum temperature of 200 °C. This fact confirmed the high susceptibility of these components to decomposition reactions, in agreement with reported data [21],

Table 2
Kinetic model proposed for autohydrolysis of galactan, regression coefficients and statistical parameters.

Kinetic model proposed for the autohydrolysis of galactan.

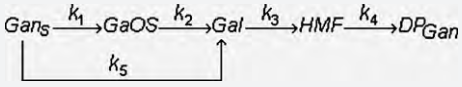

α Parameter		
α_{Gan} (dimensionless)	0.758	
Kinetic coefficient	**ln (k_{0i})[a] (k_{0i} in h^{-1})**	**E_{ai}[b] (kJ/mol)**
Arrhenius parameters		
k_1 (h^{-1})	11.9	35.9
k_2 (h^{-1})	50.2	185.9
k_3 (h^{-1})	74.2	279.5
k_4 (h^{-1})	41.2	140.8
k_5 (h^{-1})	58.9	212
Statistical parameters		
R^2 for Gan	0.950	
R^2 for GaOS	<0.9	
R^2 for Gal	0.945	
R^2 for HMF	0.925	
R^2 for DP_{Gan}	0.931	

[a] k_{0i} – preexponential factor.
[b] E_{ai} – activation energy.

which confirmed that arabinose can be decomposed into furfural upon hydrothermal processing.

3.1.4. Acetyl groups and reaction products

As it is well known, GalA units in pectins are partially acetylated. The degree of acetylation of HG is particularly high in sugar beet pectin [22]. For example, sugar beet pectin with a degree of acetylation of 33.5 mol/100 mol GalA was reported by Ralet et al. [13].

Along hydrothermal processing, acetyl groups are splitted off to yield AcH, which acts as a hydrolysis catalyst. Table 1 shows data concerning the presence of acetyl groups in solid and soluble products: the acetyl group content of the solid phase (Acn) decreased first rapidly with the severity of treatments, but at temperatures higher 167 °C varied in a narrow range (11.6–15.6%), indicating the presence of a residual, resistant fraction.

The acetyl groups linked to oligosaccharides (AcO) showed a maximum (59.3%) in the experiment performed to reach 167 °C, whereas a continuous increase in acetic acid (AcH) yield was observed. Material balances showed that AcH did not react significantly, a fact in agreement with reported studies [23].

3.2. Kinetic modeling

Based on the experimental findings, several pseudohomogeneous kinetic models (based on sequential and parallel, irreversible and first-order reactions with Arrhenius type temperature dependence) were tested to describe the SBP polysaccharide autohydrolysis (see Tables 2–5). The major polymers (Gan, An, Acn, GaUn) were assumed to be made up of two fractions (unreactive or reactive under the assayed operational conditions). The "susceptible" fractions were denoted Gan_s, An_s, Acn_s and $GaUn_s$. Polymers were first broken down into oligomers (GaOS, OGaU, AOS, AcO), and then into other soluble products. These hypotheses enabled the development of a model suitable for data interpretation. The mass ratios between the amounts of susceptible polymers and the whole amounts of the respective polymers present in the raw material (Gan_{RM}, $GaUn_{RM}$, Arn_{RM} or Acn_{RM}) were established by means of the "susceptible fractions", measured by the parameter α_i ($0 < \alpha_i < 1$

Table 3
Kinetic model proposed for autohydrolysis of galacturonan, regression coefficients and statistical parameters.

Kinetic model proposed for the autohydrolysis of galacturonan.

$GaUn_s \xrightarrow{k_6} OGaU \xrightarrow{k_7} DP_{GaUn}$

α Parameter		
α_{GaUn}	0.930	
Kinetic coefficient	**ln (k_{0i})[a] (k_{0i} in h^{-1})**	**E_{ai}[b] (kJ/mol)**
Arrhenius parameters		
k_6 (h^{-1})	9.2	24
k_7 (h^{-1})	36.7	127.5
Statistical parameters		
R^2 for GaUn	0.976	
R^2 for OGaU	0.992	
R^2 for DP_{GaUn}	0.997	

[a] k_{0i} – preexponential factor.
[b] E_{ai} – activation energy.

Table 4
Kinetic model proposed for autohydrolysis of arabinan, regression coefficients and statistical parameters.

Kinetic model proposed for the autohydrolysis of arabinan.

$An_s \xrightarrow{k_8} AOS \xrightarrow{k_9} Ara \xrightarrow{k_{10}} F \xrightarrow{k_{11}} DP_{An}$

α Parameter		
α_{An}	0.985	
Kinetic coefficient	**ln (k_{0i})[a] (k_{0i} in h^{-1})**	**E_{ai}[b] (kJ/mol)**
Arrhenius parameters		
k_8 (h^{-1})	21.1	66.5
k_9 (h^{-1})	71.9	265.9
k_{10} (h^{-1})	35.1	127.6
k_{11} (h^{-1})	21.1	68.1
Regression coefficients		
R^2 for An	0.987	
R^2 for AOS	0.993	
R^2 for Ara	0.989	
R^2 for F	<0.9	
R^2 for DP_{An}	0.941	

[a] k_{0i} – preexponential factor.
[b] E_{ai} – activation energy.

Table 5
Kinetic model proposed for autohydrolysis of acetyl groups fraction, regression coefficients and statistical parameters.

Kinetic model proposed for the autohydrolysis of acetyl groups.

$Acn_s \xrightarrow{k_{12}} AcO \xrightarrow{k_{13}} AcH$

α Parameter		
α_{Acn}	0.861	
Kinetic coefficient	**ln (k_{0i})[a] (k_{0i} in h^{-1})**	**E_{ai}[b] (kJ/mol)**
Arrhenius parameters		
k_{12} (h^{-1})	34.3	111.4
k_{13} (h^{-1})	28.8	101.2
Regression coefficients		
R^2 for Acn	0.980	
R^2 for AcO	0.989	
R^2 for AcH	0.991	

[a] k_{0i} – preexponential factor.
[b] E_{ai} – activation energy.

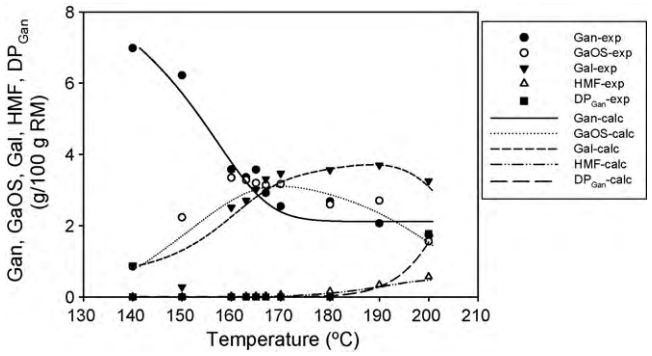

Fig. 2. Experimental (symbols) and calculated (lines) dependence of residual galactan and galactan hydrolysis products on the experimental conditions (measured by the maximum temperature of treatments).

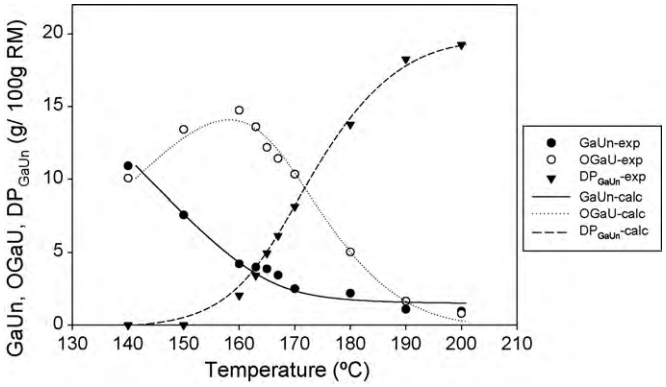

Fig. 3. Experimental (symbols) and calculated (lines) dependence of the residual galacturonan and galacturonan hydrolysis products on the experimental conditions (measured by the maximum temperature of treatments).

with i = Gan for galactan; i = GaUn for galacturonan, i = An for arabinan and i = Acn for acetyl groups).

3.2.1. Galactan

Table 2 shows the mechanism proposed for galactan autohydrolysis, based on two parallel reactions: the first one involves that the hydrolyzable galactan fraction (Gan_s) is degraded to give GaOS (which are further hydrolyzed into Gal); whereas the second one involves the direct conversion of Gan_s into Gal. This second reaction was added to the kinetic mechanism after verifying that a mechanism containing just the first reaction always predicted Gal concentrations by defect. In order to take into account Gal decomposition (confirmed from material balances), a fourth reaction dealing with the dehydration reaction of Gal to give HMF was included. Finally, it was assumed that HMF can be decomposed leading other degradation products (denoted as DP_{Gan}). Based on these considerations, the following set of equations was formulated for describing the behaviour of the Gan fraction:

$$\frac{d\,Gan_s}{dt} = -k_1 Gan_s - k_5 Gan_s \quad (1)$$

$$Gan = Gan_s + (1-\alpha_{Gan})\,Gan_{RM} \quad (2)$$

$$\alpha_{Gan} = \left.\frac{Gan_s}{Gan}\right|_{RM} \quad (3)$$

$$\frac{d\,GaOS}{dt} = k_1 Gan_s - k_2 GaOS \quad (4)$$

$$\frac{d\,Gal}{dt} = k_2 GaOS + k_5 Gan_s - k_3 Gal \quad (5)$$

$$\frac{d\,HMF}{dt} = k_3 Gal - k_4 HMF \quad (6)$$

$$DP_{Gan} = Gan_{RM} - Gan - GaOS - Gal - HMF \quad (7)$$

where k_i (i from 1 to 5) represents the kinetic coefficients. All the other parameters were defined in text, and are summarized in the list of abbreviations. Table 2 also lists the regression coefficients resulting from equation solving (susceptible fraction and Arrhenius parameters), as well as the values of R^2. The good agreement between experimental and predicted data (see Fig. 2) confirmed the suitability of the proposed equations for data interpretation.

3.2.2. Galacturonan

According to the above considerations, the kinetic mechanism proposed for the autohydrolysis of GaUn involves the formation of OGaU from the substrate and their further decomposition to degradation products (denoted DP_{GaUn}). Table 3 shows the kinetic mechanism, which led to the following set of equations:

$$\frac{d\,GaUn_s}{dt} = -k_6 GaUn_s \quad (8)$$

$$GaUn = GaUn_s + (1-\alpha_{GaUn})\,GaUn_{RM} \quad (9)$$

$$\alpha_{GaUn} = \left.\frac{GaUn_s}{GaUn}\right|_{RM} \quad (10)$$

$$\frac{d\,OGaU}{dt} = k_6 GaUn_s - k_7 OGaU \quad (11)$$

$$DP_{GaUn} = GaUn_{RM} - GaUn - OGaU \quad (12)$$

where k_i (i from 6 to 7) represents the kinetic coefficients. The rest of parameters are defined in text and included in the list of abbreviations. Table 3 shows the regression coefficients resulting from equations (α fraction and Arrhenius parameters), as well as the R^2 values. The close agreement between experimental and predicted data (see Fig. 3) confirmed the suitability of the proposed equations for data interpretation.

3.2.3. Arabinan

Table 4 shows the kinetic mechanism proposed for An, which includes a set of four sequential reactions: (i) An hydrolysis to give AOS, (ii) Ara formation from AOS, (iii) decomposition of Ara to give F and, (iv) F degradation to decomposition products (denoted DP_{An}). According to this mechanism, the set equations involved in the An autohydrolysis is:

$$\frac{d\,An_s}{dt} = -k_8 An_s \quad (13)$$

$$An = An_s + (1-\alpha_{An})\,An_{RM} \quad (14)$$

$$\alpha_{An} = \left.\frac{An_s}{An}\right|_{RM} \quad (15)$$

$$\frac{d\,AOS}{dt} = k_8 An_s - k_9 AOS \quad (16)$$

$$\frac{d\,Ara}{dt} = k_9 AOS - k_{10} Ara \quad (17)$$

$$\frac{d\,F}{dt} = k_{10} Ara - k_{11} F \quad (18)$$

$$DP_{An} = An_{RM} - An - AOS - Ara - F \quad (19)$$

where k_i (i from 8 to 11) represents the kinetic coefficients. The rest of parameters were defined in text and are included in the list of abbreviations section (see below). The values of the statistical parameters are listed in Table 4. Again, the close agreement between experimental and calculated results (see Fig. 4), confirms

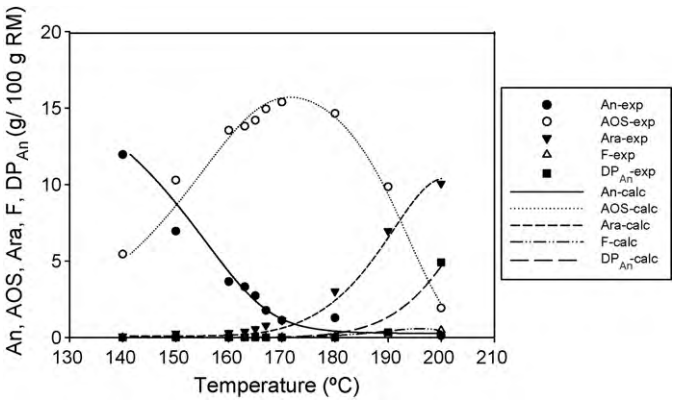

Fig. 4. Experimental (symbols) and calculated (lines) dependence of residual arabinan and arabinan hydrolysis products on the experimental conditions (measured by the maximum temperature of treatments).

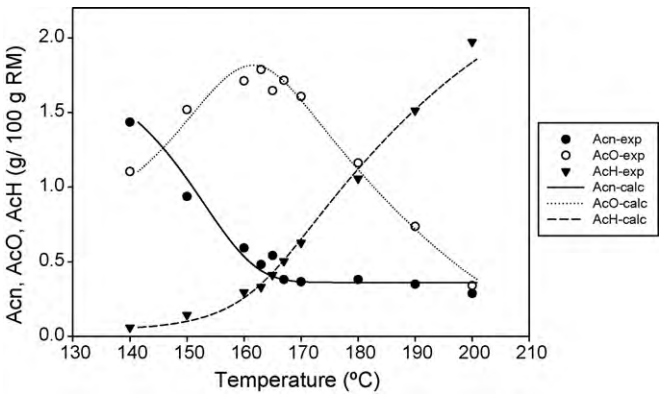

Fig. 5. Experimental (symbols) and calculated (lines) dependence of residual acetyl groups and acetyl groups hydrolysis products on the experimental conditions (measured by the maximum temperature of treatments).

the suitability of the proposed model to assess the arabinan autohydrolysis.

The high value obtained for α_{An} (0.985) confirmed the reactivity of An. According to Renard et al. [24], the glycosidic linkages between neutral sugars (Rha–Ara or Ara–Ara) are the most sensitive ones to the hydrolytic reactions in the pectic polysaccharides. On the other hand, some "simple" reactions such as Ara decomposition showed preexponential factors and activation energies in the range of the ones reported by Caparrós et al. [21] for *Arundo donax* processing.

3.2.4. Acetyl groups

The reaction pattern for Acn (Table 5) assumed that acetyl groups in solid phase (Acn_s) are first solubilized to yield acetyl groups linked to oligomeric components (AcO), and then splitted off to give AcH, which remains in the medium without further modification. Under these hypotheses, the following equations can be inferred:

$$\frac{d\,Acn_s}{dt} = -k_{12}Acn_s \quad (20)$$

$$Acn = Acn_s + (1-\alpha_{Acn})Acn_{RM} \quad (21)$$

$$\alpha_{Acn} = \left.\frac{Acn_s}{Acn}\right|_{RM} \quad (22)$$

$$\frac{d\,AcO}{dt} = k_{12}Acn_s - k_{13}AcO \quad (23)$$

$$AcH = Acn_{RM} - Acn - AcO \quad (24)$$

where k_i (i from 12 to 13) represents the kinetic coefficients. The rest of parameters were defined in text, and are summarized in the list of abbreviations.

The suitability of the proposed model for interpretation of the experimental data was demonstrated by both the values of the statistical parameters (see Table 5) and the satisfactory agreement between experimental and calculated results (see Fig. 5).

The value obtained for α_{Acn} (0.861) is about the ones determined by Yáñez et al. [23] and Caparrós et al. [21] (0.899 and 0.912 for *Acacia dealbata* and *A. donax*, respectively). Closely related values were also found for the preexponential factor and activation energy of acetyl group hydrolysis in studies dealing with *A. donax* and *A. dealbata* autohydrolysis, suggesting a kinetic behaviour independent from the type of raw material.

3.3. Selection of operational conditions and validation of the model

The interpretation of data in autohydrolysis processing has been carried out in two different ways: using the severity factor (Ro) proposed by Overend and Chornet [25], or by means of kinetic models based on multiple reactions. The severity factor, which depends on time and temperature, is useful for providing comparative data among experiments performed with different temperature profiles, and has been mentioned in the article by Martínez et al. [18]. In this work, the set of equations listed in the previous section can also be employed (with some more mathematical work) for assessing, predicting and comparing results obtained under different processing conditions (defined by time and/or temperature).

The prebiotic effect of pectin-derived oligosaccharides depends, among other factors, on the type of oligomers, their substitution pattern and their degree of polymerization. Because of this, it could be interesting to asses the production of different types of products. To this end, the kinetic models enabled the identification of operational conditions leading to reaction media containing different oligomer components. Some criteria for selecting valuable opera-

Table 6
Predicted yields according to various optimization criteria.

Parameter	Optimization criteria and selected conditions			
	Maximum GaOS production	Maximum OGaU production	Maximum AOS production	Maximum OS[a] production
Temperature (°C)	169.9	158.2	171.5	164.2
Time (h)	0.50	0.40	0.51	0.45
Product	Yields (g/100 g RM)			
AOS	15.65	12.28	15.71	14.59
OGaU	10.48	14.08	9.58	13.12
GaOS	3.10	2.54	3.10	2.97
AcO	1.59	1.77	1.51	1.79

[a] OS = AOS + OGaU + GaOS + AcO.

tional conditions are: (i) maximum GaOS production, (ii) maximum OGaU production, (iii) maximum AOS production, and (iv) maximum OS production. Table 6 shows the treatment temperatures calculated from the models, as well as the predicted compositional data for each case.

The operational conditions leading to maximum production of GaOS or AOS were very similar (maximum temperatures of 169.9 and 171.5 °C, respectively). Under these conditions, the composition of the liquors only differed slightly in OGaU production, and the AOS/OGaU ratio varied in a narrow range (1.49–1.64 g/g).

Optimum OGaU production was predicted for a significantly lower maximum temperature (158.2 °C), with a decreased AOS/OGaU ratio (0.87 g/g).

In these cases, the OS production varied in a narrow range (29.9–30.8 g/100 g SBP), whereas the maximum yield of total oligosaccharides (32.5 g OS/100 g SBP) was predicted for a treatment performed to reach 164.2 °C.

In order to validate the predictions of the kinetic model, an additional experiment was carried out at 158.2 °C. In this case, the yields of the target products (expressed as g/100 g oven-dry raw material) were: GaOS = 2.35, OGaU = 11.52, AOS = 11.1 and AcO = 1.68. Again, the suitability of the models for quantitative predictions was confirmed by the satisfactory agreement between experimental and calculated values (see predictions in Table 6). Under these operational conditions, 75.4% of the initial glucan was retained in solid phase obtaining a residue suitable to be used in a variety of applications.

4. Conclusions

Mixtures of soluble saccharides derived from sugar beet pectin were obtained by non-isothermal autohydrolysis. Based on experimental data, a kinetic model enabling the interpretation of experimental data concerning the yields in the target products was developed. Depending on the operational conditions, measured by the maximum temperature achieved in treatments, reaction media containing different proportions of oligosaccharides made up of different structural units can be obtained. According to the model predictions, when heating is kept to achieve 171.5 °C, maximum AOS yield (15.7 g AOS/100 g SBP) is obtained, at a mass ratio AOS:OGaU:GaOS:AcO of 1:0.61:0.20:0.10. Operating up to achieve 158.2 °C, OGaU is obtained at its maximum yield (14.08 g OGaU/100 g SBP). In this case the mass ratio AOS:OGaU:GaOS:AcO was 0.87:1:0.18:0.12.

Acknowledgements

Authors are grateful to the Ministry of Science and innovation of Spain (Project ref: CTQ2008-05322/PPQ, partially funded by the FEDER funds of the European Union) for the financial support of this work. R Yáñez is grateful to the Xunta de Galicia for her Isidro Parga Pondal contract.

References

[1] W.G.T. Willats, J.P. Knox, J.D. Mikkelsen, Pectin: new insights into an old polymer are starting to gel, Trends Food Sci. Technol. 17 (2006) 97–104.
[2] G. Mandalari, R.N. Bennett, R. Kirby, R. lo Curto, G. Bisignano, K.W. Waldron, C.B. Faulds, Enzymatic hydrolysis of flavonoids and pectic oligosaccharides from Bergamot (*Citrus bergamia Risso*) peel, J. Agric. Food Chem. 54 (2006) 8307–8313.
[3] M.E. Collins, R.A. Rastall, Oligosaccharides in food and Agriculture, in: B. Fraser-Reid, K. Tatsuta, J. Thiem (Eds.), Glycoscience, Springer-Verlag, Berlin Heidelberg, 2008, pp. 1185–1204.
[4] B.L. Ridley, M.A. O'Neill, D. Mohnen, Pectins: structure, biosynthesis, and oligogalacturonide-related signalling, Phytochemistry 57 (2001) 929–967.
[5] J. de Vries, in: P.A. Williams, G.O. Philips (Eds.), Gums and Stabilisers for the Food Industry, Royal Society of Chemistry, Cambridge, 2004, pp. 23–31.
[6] P.J.H. Daas, B. Boxma, A.M.C.P. Hopman, A.G.J. Voragen, H.A. Schols, Study of the methyl ester distribution in pectin with endo-polygalacturonase and high-performance size-exclusion chromatography, Biopolymers 58 (2001) 195–203.
[7] H. Yamada, H. Kiyohara, T. Matsumoto, Recent studies on possible functions of bioactive pectins and pectic polysaccharides from medicinal herbs, in: F. Voragen, H. Schols, R. Visser (Eds.), Advances in Pectin and Pectinase Research, Kluwer Academic Publishers, Dordrecht Neth, 2003, pp. 481–490.
[8] G.J. Coenen, M.A. Kabel, H.A. Schols, A.G.J. Voragen, CE–MSn of complex pectin-derived oligomers, Electrophoresis 29 (2008) 2101–2111.
[9] Available from: http://faostat.fao.org/site/339/default.aspx. Date of the last visit: 26.03.2010.
[10] M.A.H.M. Al-Tamimi, R.J. Palframan, J.M. Cooper, G.R. Gibson, R.A. Rastall, In vitro fermentation of sugar beet arabinan and arabinooligosaccharides by the human gut microflora, J. Appl. Microbiol. 100 (2006) 407–414.
[11] V.L. Finkenstadt, L. Liu, J.L. Willett, Evaluation of poly(lactic acid) and sugar beet pulp green composites, J. Polym. Environ. 15 (2007) 1–6.
[12] B.L. Foster, B.E. Dale, J.B. Doran-Peterson, Enzymatic hydrolysis of ammonia-treated sugar beet pulp, Appl. Biochem. Biotechnol. 91–93 (2001) 269–282.
[13] M.C. Ralet, J.C. Cabrera, E. Bonnin, B. Quéméner, P. Hellìn, J.F. Thibault, Mapping sugar beet pectin acetylation pattern, Phytochemistry 66 (2005) 1832–1843.
[14] V. Micard, C.M.G.C. Renard, J.F. Thibault, Enzymatic saccharification of sugar-beet pulp, Enzyme Microb. Technol. 19 (1996) 162–170.
[15] V. Micard, C.M.G.C. Renard, I.J. Colquhounb, J.F. Thibault, End-products of enzymic saccharification of beet pulp, with a special attention to feruloylated oligosaccharides, Carbohydr. Polym. 32 (1997) 285–292.
[16] P. Ferreira, N. Diez, C.B. Faulds, J. Soliveri, J.L. Copa-Patiño, Release of ferulic acid and feruloylated oligosaccharides from sugar beet pulp by *Streptomyces tendae*, Bioresour. Technol. 98 (2007) 1522–1528.
[17] K.M.J. Van Laere, R. Hartemink, M. Bosveld, H.A. Schols, A.G.J. Voragen, Fermentation of plant cell wall derived polysaccharides and their corresponding oligosaccharides by intestinal bacteria, J. Agric. Food Chem. 48 (2000) 1644–1652.
[18] M. Martínez, B. Gullón, H.A. Schols, J.L. Alonso, J.C. Parajó, Assessment on the production of oligomeric compounds from sugar beet pulp, J. Agric. Food Chem. 48 (2009) 4681–4687.
[19] M.J. González-Muñóz, H. Dominguez, J.C. Parajó, Depolymerization of xylan-derived products in an enzymatic membrane reactor, J. Membr. Sci. 320 (2008) 224–231.
[20] N. Blumenkrantz, G. Asboe-Hansen, New method for quantitative determination of uronic acids, Anal. Biochem. 54 (1973) 484–489.
[21] S. Caparrós, G. Garrote, J. Ariza, F. López, Autohydrolysis of *Arundo donax* L., a kinetic assessment, Ind. Eng. Chem. Res. 45 (2006) 8909–8920.
[22] W.G.T. Willats, L. McCartney, W. Mackie, J.P. Knox, Pectin: cell biology and prospects for functional analysis, Plant Mol. Biol. 47 (2001) 9–27.
[23] R. Yáñez, A. Romaní, G. Garrote, J.L. Alonso, J.C. Parajó, Processing of *Acacia dealbata* in aqueous media: a first step of wood biorefinery, Ind. Eng. Chem. Res. 48 (2009) 6618–6626.
[24] C.M.G.C. Renard, M.J. Crépeau, J.F. Thibault, Structure of the repeating units in the rhamnogalacturonic backbone of apple, beet and citrus pectins, Carbohydr. Res. 275 (1995) 155–165.
[25] R.P. Overend, E. Chornet, Heavy-oil cracking – the case for nonhomogenous kinetics, Can. J. Phys. 68 (1990) 1105–1111.